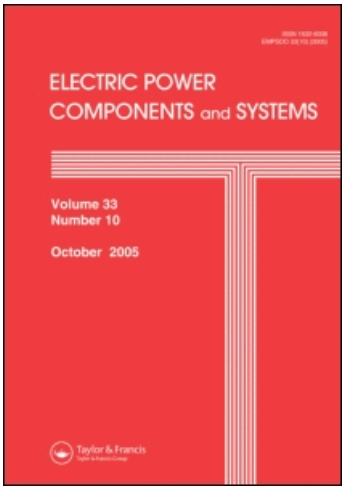

Electric Power Components and Systems
Publication details, including instructions for authors and subscription information:
http://www.informaworld.com/smpp/title~content=t713399721

A Generalized Heffron-Phillips Model for Multi-Machine Power Systems with Voltage and Frequency Dependent Loads

M. Hasan Modir Shanechi; Majid Oloomi Buygi

Online publication date: 29 October 2010

To cite this Article Shanechi, M. Hasan Modir and Buygi, Majid Oloomi(2001) 'A Generalized Heffron-Phillips Model for Multi-Machine Power Systems with Voltage and Frequency Dependent Loads', Electric Power Components and Systems, 29: 5, 389 — 404
To link to this Article: DOI: 10.1080/15325000151133523
URL: http://dx.doi.org/10.1080/15325000151133523

Electric Power Components and Systems, 29:389–404, 2001

1532-5008/01 $12.00 + .00

A Generalized Heffron-Phillips Model for Multi-Machine Power Systems with Voltage and Frequency Dependent Loads

M. HASAN MODIR SHANECHI
MAJID OLOOMI BUYGI

Department of Electrical Engineering
Ferdowsi University
Mashhad, Iran

In this paper the multi-machine Heffron-Phillips model is generalized to handle multi-machine power systems with frequency and voltage-dependent loads. A systematic method for extracting state equations is proposed which preserves structure and is able to account for infinite bus directly. The generalized model's block diagram is similar to that of Heffron-Phillips and is suitable for generalizing dynamic studies of networks with impedance loads to networks with frequency- and voltage-dependent loads. Two applications of this model are presented: (1) studying effects of load model parameters on dynamic stability of a five-bus network, and (2) designing a PSS for a one-machine infinite bus with frequency- and voltage-dependent local load and comparing it with a PSS designed based on impedance load.

1 Introduction

In 1952, Heffron and Phillips [1] presented a simplified linear model for a synchronous machine connected to an infinite bus with a local impedance load. Thereafter, this model has been used extensively in power system dynamic analysis. The small perturbation stability characteristic of a single machine supplying an infinite bus was explored by means of frequency response analysis [2] by de Mello and Concordia. De Mello and Laskowski used this model to find the system configurations and loading conditions that produce negative damping [3]. This model was later generalized for multi-machine power systems [4] and was widely used to study means of increasing damping and coordinating PSS's via the supplementary excitation control [4–10].

In all of the above investigations, loads were considered as impedances. In reality, loads are voltage- and frequency-dependent. Many mathematical representations, such as constant impedance, constant current, constant power, polynomial, exponential, EPRI LOADSYN, and EPRI ETMSP, were proposed for load modeling [11–14]. Brucoli et al. [15] proposed a new procedure for analyzing the effects of static load modeling on the voltage stability limits. They used a static frequency–dependent load for this purpose. Kao et al. [16] proposed that using a composite

Manuscript received in final form on July 28, 2000.
Address correspondence to M. Hasan Modir Shanechi.

load model (static and dynamic) provides a more accurate representation than other models. A bibliography on load models for power flow and dynamic performance was presented in [17]. Two kinds of dynamic load model, including a single-motor model and a two-motor model, was developed for the stability study of Taiwan power system by Kao et al. [18]. Multiple load types were recommended for transient stability, long-term dynamics, and small perturbation stability in [19]. The interaction between the load and the power system was explored in terms of load and system transfer function by Hiskens and Milanovic [20]. Khodabakhchian and Vuong [21] developed an EMTP model for a mixed residential-commercial load, which is valid for large voltage variations; they established guidelines for modeling this type of load in dynamic studies such as first swing, transient, and voltage stability. A simple model for air conditioner load for power system studies was developed by Tomiyama et al. [22]. A simplified linear state space model for a multi-machine power system with frequency- and voltage-dependent loads has been developed by Bhatti and Hill [23], wherein resistance and parallel admittance of transmission lines have been ignored. Their proposed block diagram is not similar to Heffron-Phillips's block diagram. They have assumed that each bus has a frequency-dependent load, hence all bus voltage angles are considered as state variables. In practice, many buses do not have loads or their loads are not frequency dependent, so their voltage angles are not state variables.

In this paper a new systematic approach for modeling power system networks with frequency and voltage-dependent loads is presented. This approach assumes that each generator terminal bus and also each purely load bus may or may not have frequency- and voltage-dependent loads. Power balance is used at each bus for system modeling.

In modeling power systems with infinite bus, usually the infinite bus is considered as a large generator. This increases the dimensions of the matrices used in the calculations of the linear model. A direct method to account for the infinite bus is developed and used in this paper which overcomes this shortcoming.

Basic assumptions for system modeling are explained in Section 2. State equations are derived in Subsections 2.1 and 2.2. In Subsection 2.3, generalized Heffron-Phillips model coefficients and its block diagram are derived. A direct method to account for infinite bus is proposed in Subsection 2.4. The effects of frequency and voltage dependence of the load on the dynamic behaviour of a five-bus example system is explored in Subsection 3.1. In Subsection 3.2 a PSS is designed for one machine infinite bus system with frequency- and voltage-dependent local load and is compared with the PSS designed based on impedance load.

2 System Modeling

In an n bus power system, it is assumed that the power system consists of n_g generator terminal buses (GTB) and n_l purely load buses (PLB). Each GTB or PLB may have frequency-dependent loads (FL). Assuming:

n_{gf} = number of GTBs with FL (bus type no. 1)
n_{gn} = number of GTBs without FL (bus type no. 2)
n_{lf} = number of PLBs with FL (bus type no. 3)
n_{ln} = number of PLBs without FL (bus type no. 4)

Bus type nos. 1, 2, 3, and 4 are numbered in sequence. Each load is modeled with a general function of voltage and frequency:

$$P_{di} = f_i^p(\omega_i, v_i),$$
$$Q_{di} = f_i^q(\omega_i, v_i), \tag{1}$$

where P_{di}, Q_{di}, ω_i, and v_i are active load, reactive load, frequency, and voltage of the ith bus in p.u. Figure 1 shows the phasor diagram of the ith GTB and jth PLB in transient state with a common synchronously rotating reference frame. From this figure, it is clear that

$$\dot{\theta}_k = \omega_o \omega_k, \tag{2}$$

where θ_k is the voltage angle of kth bus in radian and ω_o is the base angular frequency in rad/sec. "Simplified dynamic model" is used for each generator with four state variables $\Delta\delta$, $\Delta\omega$, $\Delta E'$, ΔE_{fd} [1], and each frequency-dependent load is modeled with a state variable $\Delta\theta$ [23]. Power flow equations (PFE) are used for extracting state equations of new state variables ($\Delta\theta$). PFEs for the ith bus are [24]

$$P_i = P_{gi} - P_{di} = \sum_{k=1}^{n} v_i v_k y_{ik} \cos(\theta_k - \theta_i + \gamma_{ik}),$$
$$Q_i = Q_{gi} - Q_{di} = -\sum_{k=1}^{n} v_i v_k y_{ik} \sin(\theta_k - \theta_i + \gamma_{ik}), \qquad i = 1, \ldots, n, \tag{3}$$

where P_{gi} and Q_{gi} are active and reactive power generation, and P_i and Q_i are the active and reactive power injections at the ith bus, respectively. The dynamic equations ($\dot{X} = AX + BU$, $Y = CX + DU$) for power systems with voltage- and frequency-dependent loads are derived in Section 2. In Subections 2.1 and 2.2, the new state equations are derived by linearizing (3) and omitting nonstate variables. Matrices A and B can be derived by adding the new state equations to simplified dynamic model. In Subsection 2.3, the outputs ΔP_{gi}, Δv_i, and ΔE_i are written versus state variables, and matrices C and D are derived.

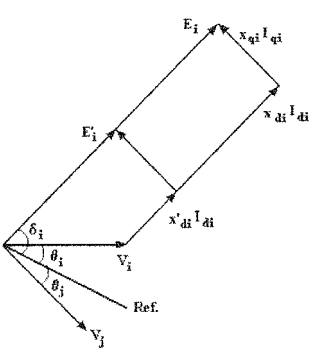

Figure 1. Phasor diagram of ith and jth buses.

2.1 PFEs for PLBs

At PLBs, power generation is zero ($P_{gi} = 0, Q_{gi} = 0$), therefore, for the ith PLB, PFEs are

$$\sum_{k=1}^{n} v_i v_k y_{ik} \cos(\theta_k - \theta_i + \gamma_{ik}) = -f_i^p(\dot{\theta}_i, v_i)$$

$$-\sum_{k=1}^{n} v_i v_k y_{ik} \sin(\theta_k - \theta_i + \gamma_{ik}) = -f_i^q(\dot{\theta}_i, v_i), \qquad i = \mathrm{n_g} + 1, \ldots, n. \tag{4}$$

Linearizing equation (4) yields

$$\begin{bmatrix} M\,1_{l.g} & N\,1_{l.g} & N\,1_{l.l} \\ m\,2_{l.g} & N\,2_{l.g} & N\,2_{l.l} \end{bmatrix} \begin{bmatrix} \Delta V_g \\ \Delta \theta_g \\ \Delta \theta_l \end{bmatrix} = \begin{bmatrix} -M\,1_{l.l} & T1_{l.l} \\ -M\,2_{l.l} & T2_{l.l} \end{bmatrix} \begin{bmatrix} \Delta V_l \\ \Delta \dot{\theta}_l \end{bmatrix}, \tag{5}$$

where

$$\Delta V_g = [\Delta v_1, \cdots, \Delta v_{ng}]^T, \qquad \Delta \theta_l = [\Delta \theta_{ng+1}, \cdots, \Delta \theta_n]^T,$$
$$\Delta \theta_g = [\Delta \theta_1, \cdots, \Delta \theta_{ng}]^T, \qquad \Delta \dot{\theta}_l = [\Delta \dot{\theta}_{ng+1}, \cdots \Delta \dot{\theta}_n]^T,$$
$$\Delta V_l = [\Delta v_{ng+1}, \cdots, \Delta v_n]^T,$$

and the elements of the submatrices can be easily computed by linearizing (4) [25]. In this paper, letters M, N, R, S, and T are used to represent the matrices multiplying the vectors ΔV, $\Delta \theta$, $\Delta \delta$, $\Delta E'$, and $\Delta \dot{\theta}$, respectively. Active and reactive PFEs are distinguished by numbers 1 and 2, respectively. Each submatrix has two subscripts: the left subscript denotes the bus type of the PFE and the right subscript denotes the bus type of its multiplier vector. The subscript of each vector denotes the bus type of its elements. Subscripts g, l, gf, gn, lf, ln denote GTBs, PLBs, bus type nos. 1, 2, 3, and 4, respectively.

If all PLBs have active or reactive FLs ($\mathrm{n_1} = \mathrm{n_{lf}}, \mathrm{n_{ln}} = 0$), the variables Δv_i and $\Delta \dot{\theta}_j$ will be independent for $i = \mathrm{n_g} + 1, \ldots, \mathrm{n}, j = \mathrm{n_g} + 1, \ldots, \mathrm{n}$, then the right-hand side matrix of (5) is invertible, and ΔV_{lf}, $\Delta \dot{\theta}_{lf}$ can be calculated in terms of other variables. In case some PLBs do not have active and reactive FL ($\mathrm{n_{ln}} \neq 0$), column k of $T1_{l.l}$ and $T2_{l.l}$ are zero for $k = \mathrm{n_g} + \mathrm{n_{lf}} + 1, \ldots, \mathrm{n}$, and the right-hand side matrix of (5) is not invertible. In this case, for calculating ΔV_{lf} and $\Delta \dot{\theta}_{lf}$, ΔV_{ln} and $\Delta \theta_{ln}$ must be calculated from PFEs of PLBs without FL in terms of other variables and substituted into PFEs of PLBs with FL. Partitioning (5) into PFEs of PLBs with FL and PFEs of PLBs without FL yields

$$\begin{bmatrix} M\,1_{lf.g} & N\,1_{lf.g} & N\,1_{lf.lf} & M\,1_{lf.ln} & N\,1_{lf.ln} \\ M\,2_{lf.g} & N\,2_{lf.g} & N\,2_{lf.lf} & M\,2_{lf.ln} & N\,2_{lf.ln} \end{bmatrix} \begin{bmatrix} \Delta V_g \\ \Delta \theta_g \\ \Delta \theta_{lf} \\ \Delta V_{ln} \\ \Delta \theta_{ln} \end{bmatrix}$$

$$= \begin{bmatrix} -M\,1_{lf.lf} & T1_{lf.lf} \\ -M\,2_{lf.lf} & T2_{lf.lf} \end{bmatrix} \begin{bmatrix} \Delta V_{lf} \\ \Delta \dot{\theta}_{lf} \end{bmatrix}, \tag{6}$$

$$\begin{bmatrix} M\,1_{ln.g} & N\,1_{ln.g} & M\,1_{ln.lf} & N\,1_{ln.lf} \\ M\,2_{ln.g} & N\,2_{\ln.g} & M\,2_{ln.lf} & N\,2_{ln.lf} \end{bmatrix} \begin{bmatrix} \Delta V_g \\ \Delta \theta_g \\ \Delta V_{lf} \\ \Delta \theta_{lf} \end{bmatrix}$$

$$= \begin{bmatrix} -M\,1_{ln.ln} & -N\,1_{ln.ln} \\ -M\,2_{ln.ln} & -N\,2_{ln.ln} \end{bmatrix} \begin{bmatrix} \Delta V_{ln} \\ \Delta \theta_{ln} \end{bmatrix}. \tag{7}$$

Computing ΔV_{ln} and $\Delta \theta_{ln}$ from (7), substituting them into (6) and computing ΔV_{lf} and $\Delta \dot{\theta}_{lf}$, and finally computing ΔV_{ln} and $\Delta \theta_{ln}$ in terms of ΔV_g, $\Delta \theta_g$, $\Delta \theta_{lf}$ by substituting ΔV_{lf} from the last equation yields

$$\begin{bmatrix} \Delta V_{lf} \\ \Delta \dot{\theta}_{lf} \end{bmatrix} = \begin{bmatrix} M'1_{lf.g} & N'1_{lf.g} & N'1_{lf.lf} \\ M'2_{lf.g} & N'2_{lf.g} & N'2_{lf.lf} \end{bmatrix} \begin{bmatrix} \Delta V_g \\ \Delta \theta_g \\ \Delta \theta_{lf} \end{bmatrix}, \tag{8}$$

$$\begin{bmatrix} \Delta V_{ln} \\ \Delta \theta_{ln} \end{bmatrix} = \begin{bmatrix} M'1_{ln.g} & N'1_{ln.g} & N'1_{ln.lf} \\ M'2_{ln.g} & N'2_{ln.g} & N'2_{ln.lf} \end{bmatrix} \begin{bmatrix} \Delta V_g \\ \Delta \theta_g \\ \Delta \theta_{lf} \end{bmatrix}, \tag{9}$$

where the above submatrices can be easily computed by linear algebra.

2.2 PFE for GTBs

At GTBs, power generation is given by

$$\begin{aligned} P_{gi} &= \frac{v_i E'_i}{x'_{di}} \sin(\delta_i - \theta_i) + \frac{v_i^2}{2}\left(\frac{1}{x_{qi}} - \frac{1}{x'_{di}}\right)\sin 2(\delta_i - \theta_i), \\ Q_{gi} &= \frac{v_i E'_i \cos(\delta_i - \theta_i) - v_i^2}{x'_{di}} - v_i^2\left(\frac{1}{x_{qi}} - \frac{1}{x'_{di}}\right)\sin^2(\delta_i - \theta_i); \end{aligned} \tag{10}$$

substituting (10) and (1) in (3), linearizing, and regrouping yields

$$\begin{bmatrix} R\,1_{g.g} & S\,1_{g.g} & M\,1_{g.l} & N\,1_{g.g} & N\,1_{g.l} \\ R\,2_{g.g} & S\,2_{g.g} & M\,2_{g.l} & N\,2_{g.g} & N\,2_{g.l} \end{bmatrix} \begin{bmatrix} \Delta E'_g \\ \Delta \delta_g \\ \Delta V_l \\ \Delta \theta_g \\ \Delta \theta_l \end{bmatrix} = \begin{bmatrix} -M\,1_{g.g} & T1_{g.g} \\ -M\,2_{g.g} & T2_{g.g} \end{bmatrix} \begin{bmatrix} \Delta V_g \\ \Delta \dot{\theta}_g \end{bmatrix}, \tag{11}$$

where

$$\Delta E'_g = [\Delta E'_1, \ldots, \Delta E'_{ng}]^T, \qquad \Delta \delta_g = [\Delta \delta_1, \ldots, \Delta \delta_{ng}]^T,$$

$$\Delta \dot{\theta}_g = [\Delta \dot{\theta}_1, \ldots, \Delta \dot{\theta}_{ng}]^T,$$

and the elements of the submatrices can be easily computed by linearizing (10) [25]. Substituting for ΔV_{lf} from (8) and for ΔV_{ln} and $\Delta \theta_{ln}$ from (9) into (11) yields

$$\begin{bmatrix} R\,1_{g.g} & S\,1_{g.g} & N'1_{g.g} & N'1_{g.lf} \\ R\,2_{g.g} & S\,2_{g.g} & N'2_{g.g} & N'2_{g.lf} \end{bmatrix} \begin{bmatrix} \Delta E'_g \\ \Delta \delta_g \\ \Delta \theta_g \\ \Delta \theta_{lf} \end{bmatrix} = \begin{bmatrix} -M'1_{g.g} & T1_{g.g} \\ -M'2_{g.g} & T2_{g.g} \end{bmatrix} \begin{bmatrix} \Delta V_g \\ \Delta \dot{\theta}_g \end{bmatrix}, \tag{12}$$

where the above submetrics can be easily computed by linear algebra. If all GTBs have active or reactive frequency-dependent loads ($n_g = n_{gf}, n_{gn} = 0$), the right-hand side matrix of (12) is invertible, and ΔV_{gf}, $\Delta \dot{\theta}_{gf}$ can be calculated in terms of other variables. In case some GTBs do not have active and reactive frequency-dependent loads ($n_{ln} \neq 0$), ΔV_{gn} and $\Delta \theta_{gn}$ are calculated from PFEs of GTBs without FL in terms of other variables and substituted into PFEs of GTBs with FL. Partitioning (12) yields

$$\begin{bmatrix} R1_{gf.g} & S1_{gf.g} & N'1_{gf.gf} & M'1_{gf.gn} & N'1_{gf.gn} & N'1_{gf.lf} \\ R2_{gf.g} & S2_{gf.g} & N'2_{gf.gf} & M'2_{gf.gn} & N'2_{gf.gn} & N'2_{gf.lf} \end{bmatrix} \begin{bmatrix} \Delta E'_g \\ \Delta \delta_g \\ \Delta \theta_{gf} \\ \Delta V_{gn} \\ \Delta \theta_{gn} \\ \Delta \theta_{lf} \end{bmatrix}$$

$$= \begin{bmatrix} -M'1_{gf.gf} & T1_{gf.gf} \\ -M'2_{gf.gf} & T2_{gf.gf} \end{bmatrix} \begin{bmatrix} \Delta V_{gf} \\ \Delta \dot{\theta}_{gf} \end{bmatrix}, \tag{13}$$

$$\begin{bmatrix} R1_{gn.g} & S1_{gn.g} & M'1_{gn.gf} & N'1_{gn.gf} & N'1_{gn.lf} \\ R2_{gn.g} & S2_{gn.g} & M'2_{gn.gf} & N'2_{gn.gf} & N'2_{gn.lf} \end{bmatrix} \begin{bmatrix} \Delta E'_g \\ \Delta \delta_g \\ \Delta V_{gf} \\ \Delta \theta_{gf} \\ \Delta \theta_{lf} \end{bmatrix}$$

$$= \begin{bmatrix} -M'1_{gn.gn} & -N'1_{gn.gn} \\ -M'2_{gn.gn} & -N'2_{gn.gn} \end{bmatrix} \begin{bmatrix} \Delta V_{gn} \\ \Delta \theta_{gn} \end{bmatrix}. \tag{14}$$

Computing ΔV_{gn} and $\Delta \theta_{gn}$, ΔV_{gf} and $\Delta \dot{\theta}_{gf}$ from (13) and (14) in terms of $\Delta E'_g$, $\Delta \delta_g$, $\Delta \theta_{gf}$, $\Delta \theta_{lf}$ yields

$$\begin{bmatrix} \Delta V_{gf} \\ \Delta \dot{\theta}_{gf} \end{bmatrix} = \begin{bmatrix} R''1_{gf.g} & S''1_{gf.g} & N''1_{gf.gf} & N''1_{gf.lf} \\ R''2_{gf.g} & S''2_{gf.g} & N''2_{gf.gf} & N''2_{gf.lf} \end{bmatrix} \begin{bmatrix} \Delta E'_g \\ \Delta \delta_g \\ \Delta \theta_{gf} \\ \Delta \theta_{lf} \end{bmatrix}, \tag{15}$$

$$\begin{bmatrix} \Delta V_{gn} \\ \Delta \theta_{gn} \end{bmatrix} = \begin{bmatrix} R''1_{gn.g} & S''1_{gn.g} & N''1_{gn.gf} & N''1_{gn.lf} \\ R''2_{gn.g} & S''2_{gn.g} & N''2_{gn.gf} & N''2_{gn.lf} \end{bmatrix} \begin{bmatrix} \Delta E'_g \\ \Delta \delta_g \\ \Delta \theta_{gf} \\ \Delta \theta_{lf} \end{bmatrix}, \tag{16}$$

where the above submetrics can be easily computed by linear algebra. Substituting for ΔV_{gf}, ΔV_{gn}, $\Delta \theta_{gn}$ from (15), and (16) into (8), yields

$$\Delta \dot{\theta}_{lf} = [R''2_{lf.g} \quad S''2_{lf.g} \quad N''2_{lf.gf} \quad N''2_{lf.lf}] \begin{bmatrix} \Delta E'_g \\ \Delta \delta_g \\ \Delta \theta_{gf} \\ \Delta \theta_{lf} \end{bmatrix}, \tag{17}$$

where the above submetrics can be easily computed by linear algebra. The new state equations are given in (15) and (17).

2.3 Coefficients Calculation

In power system with FLs, state variables are $[\Delta\delta_g, \Delta\omega_g, \Delta E'_g, \Delta E_{fd}, \Delta\theta_{gf}, \Delta\theta_{lf}]$. Writing ΔP_{gi}, Δv_i, and ΔE_i as a linear combination of these state variables:

$$\Delta P_{gi} = \sum_{m=1}^{ng}(k1)_{im}.\Delta\delta_m + \sum_{m=1}^{ng}(k2)_{im}.\Delta E'_m + \sum_{m=1}^{ngf}(k'1)_{im}.\Delta\theta_m + \sum_{m=1}^{nlf}(k''1)_{im}.\Delta\theta_{m+ng}, \tag{18}$$

$$\Delta E_i = \sum_{m=1}^{ng}(k4)_{im}.\Delta\delta_m + \sum_{m=1}^{ng}\frac{1}{(k3)_{im}}.\Delta E'_m + \sum_{m=1}^{ngf}(k'4)_{im}.\Delta\theta_m + \sum_{m=1}^{nlf}(k''4)_{im}.\Delta\theta_{m+ng}, \tag{19}$$

$$\Delta v_i = \sum_{m=1}^{ng}(k5)_{im}.\Delta\delta_m + \sum_{m=1}^{ng}(k6)_{im}.\Delta E'_m + \sum_{m=1}^{ngf}(k'5)_{im}.\Delta\theta_m + \sum_{m=1}^{nlf}(k''5)_{im}.\Delta\theta_{m+ng}, \tag{20}$$

From (15), (17), (18), (19), (20), and simplified dynamic model, the block diagram of Figure 2 will be derived. System matrices A, B, C, and D can be easily derived from Figure 2. What remains is calculating coefficients $\mathbf{K}$. Linearizing (10) yields

$$\Delta P_g = [R\,p_{g.g} \quad S\,p_{g.g} \quad M\,p_{g.g} \quad N\,p_{g.g}] \begin{bmatrix} \Delta E'_g \\ \Delta\delta_g \\ \Delta V_g \\ \Delta\theta_g \end{bmatrix}. \tag{21}$$

The elements of the submatrices are easily computable. Substituting for ΔV_g and $\Delta\theta_{gn}$ from (15) and (16) in (21) yields

$$\Delta P_g = [K2 \quad K1 \quad K'1 \quad K''1] \begin{bmatrix} \Delta E''_g \\ \Delta\delta_g \\ \Delta\theta_{gf} \\ \Delta\theta_{lf} \end{bmatrix}, \tag{22}$$

where

$$\begin{aligned} K2 &= R\,p_{g.g} + M\,p_{g.g}.R''1_{g.g} + N\,p_{g.gn}.R''2_{gn.g}, \\ K1 &= S\,p_{g.g} + M\,p_{g.g}.S''1_{g.g} + N\,p_{g.gn}.S''2_{gn.g}, \\ K'1 &= N\,p_{g.gf} + M\,p_{g.g}.N''1_{g.gf} + N\,p_{g.gn}.N''2_{gn.gf}, \\ K''1 &= M\,p_{g.g}.N''1_{g.lf} + N\,p_{g.gn}.N''2_{gn.lf}. \end{aligned} \tag{23}$$

From the phasor diagram of Figure 1:

$$E_i = \frac{x_{di}}{x'_{di}}E'_i + \left(1 - \frac{x_{di}}{x'_{di}}\right)\mathrm{v}_i\cos(\delta_i - \theta_i). \tag{24}$$

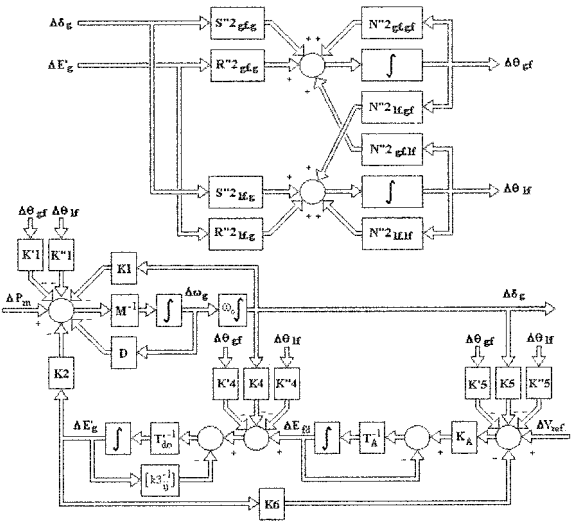

Figure 2. Block diagram of multi-machine power systems with frequency dependent loads.

Linearizing (24) and substituting for Δv_i from (15) and (16), and $\Delta \theta_i$ (for $i > n_{gf}$) from (16) yields, for $i \leq n_{gf}$:

$$\begin{aligned}
(k3)_{ij} &= L_{3i}.(r''1_{gf.g})_{ij}, \quad i \neq j, \qquad (k3)_{ii} = [L_{3i}.(r''1_{gf.g})_{ii} + L_{1i}]^{-1}, \\
(k4)_{ij} &= L_{3i}.(s''1_{gf.g})_{ij}, \quad i \neq j, \qquad (k4)_{ii} = L_{3i}.(s''1_{gf.g})_{ii} + L_{2i}], \\
(k'4)_{ij} &= L_{3i}.(n''1_{gf.gf})_{ij}, \quad i \neq j, \qquad (k'4)_{ii} = L_{3i}.(n''1_{gf.gf})_{ii} - L_{2i}, \\
(k''4)_{ij} &= L_{3i}.(n''1_{gf.lf})_{ij-n_g};
\end{aligned} \tag{25}$$

and for $i > n_{gf}$:

$$\begin{aligned}
(k3)_{ij} &= [L_{3i}.(r''1_{gn.g})_{i-n_{gf}j} - L_{2i}.(r''2_{gn.g})_{i-n_{gf}j}]^{-1}, \quad i \neq j, \\
(k3)_{ii} &= [L_{3i}.(r''1_{gn.g})_{i-n_{gf}i} - L_{2i}.(r''2_{gn.g})_{i-n_{gf}i} + L_{1i}]^{-1}, \\
(k4)_{ij} &= L_{3i}.(s''1_{gn.g})_{i-n_{gf}j} - L_{2i}.(s''2_{gn.g})_{i-n_{gf}j}, \qquad i \neq j, \\
(k4)_{ii} &= L_{3i}.(s''1_{gn.g})_{i-n_{gf}i} - L_{2i}.(s''2_{gn.g})_{i-n_{gf}i} + L_{2i}, \\
(k'4)_{ij} &= L_{3i}.(n''1_{gn.gf})_{i-n_{gf}j} - L_{2i}.(n''2_{gn.gf})_{i-n_{gf}j}, \\
(k''4)_{ij} &= L_{3i}.(n''1_{gn.lf})_{i-n_{gf}j-n_g} - L_{2i}.(n''2_{gn.lf})_{i-n_{gf}j-n_g},
\end{aligned} \tag{26}$$

where

$$L_{1i} = \left(\frac{x_{di}}{x'_{di}}\right), \quad L_{2i} = \left(\frac{x_{di}}{x'_{di}} - 1\right) v_i^o \sin(\delta_i^o - \theta_i^o), \quad L_{3i} = \left(1 - \frac{x_{di}}{x'_{di}}\right) \cos(\delta_i^o - \theta_i^o).$$

Combining (15) and (16) yields

$$\Delta V_g = [R''1_{g.g} \quad S''1_{g.g} \quad N''1_{g.gf} \quad N''1_{g.lf}] \begin{bmatrix} \Delta E'_g \\ \Delta \delta_g \\ \Delta \theta_{gf} \\ \Delta \theta_{lf} \end{bmatrix}.$$

Then

$$K5 = S''1_{g.g}, \quad K6 = R''1_{g.g}, \quad K'5 = N''1_{g,gf}, \quad K''5 = N''1_{g.lf}. \tag{27}$$

2.4 Accounting For Infinite Bus

When bus no. k is an infinite bus, the variables $\Delta E'_k$, Δv_k, $\Delta \delta_k$, $\Delta \theta_k$, $\Delta \dot{\theta}_k$ and their derivations are zero; therefore, row k of vectors $\Delta E'_g$, $\Delta \delta_g$, ΔV_g, $\Delta \theta_g$, $\Delta \dot{\theta}_g$, column k of submatrices $M\, i_{l.g}$, $N\, i_{l.g}$, and row and column k of submatrices $R\, i_{g.g}$, $S\, i_{g.g}$, $M\, i_{g.g}$, $N\, i_{g.g}$, $T i_{g.g}$ for $i = 1, 2$ in (5) and (11) are omitted.

3 Applications

The proposed model is suitable for generalizing dynamic studies of networks with impedance loads to networks with frequency- and voltage-dependent loads. It can be used for designing PSS, coordinating PSSs, determining optimal place for PSSs, and determining the effects of loads on dynamic stability, in a power system with frequency- and voltage-dependent loads.

3.1 Effects of Load Model Parameters on Dynamic Stability

The five-bus study system is shown in Figure 3, and its parameters and operating point are given in Appendix A. The load at bus No. 4 will have one of the following models:

1. EPRI LOADSYN static load model [12]:

$$\begin{aligned} p_{d4} &= f^{\mathrm{p}}(v_4, \omega_4) = k_p v_4^{kpv}[1 + k_{p\omega}(\omega - 4 - 1)], \\ q_{d4} &= f^{\mathrm{q}}(v_4, \omega_4) = k_q v_4^{kqv}[1 + k_{q\omega}(\omega_4 - 1)]. \end{aligned} \tag{28}$$

2. Exponential load model [11]:

$$\begin{aligned} p_{d4} &= f^{\mathrm{p}}(v_4, \omega_4) = k_p v_4^{kpv} \omega_4^{kp\omega}, \\ q_{d4} &= f^{\mathrm{q}}(v_4, \omega_4) = k_q v_4^{kqv} \omega_4^{kq\omega}. \end{aligned} \tag{29}$$

When the load parameters change, the magnitude of active and reactive loads will change. The magnitudes of loads, as well as their power factor, will, in turn, affect the location of eigenvalues. To show only the effects of load model parameters on the locations of critical eigenvalues, magnitude and power factor of loads are kept constant by adjusting the coefficients kp and kq, as the parameters kpv, $kp\omega$, kqv, or

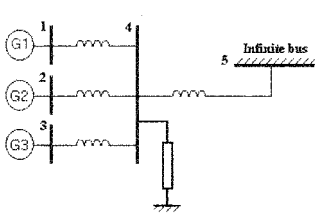

Figure 3. Five-bus study system.

Table 1
Characteristics of loads of bus no. 4 for different cases

Case	Load model	kv	$k\omega$	ω	Fig.
1	L. SYN	2	Variable	0.9	4
2	Exp.	2	Variable	0.9	5
3	L. SYN and Exp.	Variable	1	1	6

$kq\omega$ change. The locus of dominant eigenvalues were drawn for the cases of Table 1 in Figures 4–6 (in all cases, $kpv = kqv = kv$, $kp\omega = kq\omega = k\omega$).

All elements of all submatrices in (5) and (11), except elements of $T1_{l.l}$, $T2_{l.l}$, $M\ 1_{l.l}$, and $M\ 2_{l.l}$ remain constant as $k\omega$ or kv change. Therefore, locations of eigenvalues depend on these elements. These matrices are 1 by 1 in this example. For LOADSYN model:

$$t1_{ll} = -\frac{p_{d4}}{\omega_b}\frac{k_\omega}{1 + k_\omega(\omega_4 - 1)}, \qquad t2_{ll} = \frac{q_{d4}}{\omega_b}\frac{k_\omega}{1 + k_\omega(\omega_4 - 1)},$$
$$m1_{ll} = C_1 + p_{d4}\frac{k_v}{v_4}, \quad C_1 = cte, \qquad m1_{ll} = C_2 + p_{d4}\frac{k_v}{v_4}, \quad C_2 = cte; \tag{30}$$

and for exponential model:

$$t1_{ll} = \frac{p_{d4}}{\omega_b}\frac{k_\omega}{\omega_4}, \qquad t2_{ll} = \frac{q_{d4}}{\omega_b}\frac{k_\omega}{\omega_4},$$
$$m1_{ll} = C_1 + p_{d4}\frac{k_v}{v_4}, \quad C_1 = cte, \qquad m2_{ll} = C_2 + q_{d4}\frac{k_v}{v_4}, \quad C_2 = cte. \tag{31}$$

Equations (30) and (31) and Figures 4 and 5 show that in cases 1 and 2, $m1_{ll}$ and $m2_{ll}$ remain constant, $t1_{ll}$ and $t2_{ll}$ decrease, and critical eigenvalues move toward the left of imaginary axis as $k\omega$ increases; hence, the location of eigenvalues depend only on the values of $t1_{ll}$ and $t2_{ll}$.

Equations (30) and (31) also show that the rate of decrease of $t1_{ll}$ and $t2_{ll}$, as $k\omega$ increases, will be increased (decreased) in lower (higher) frequencies. Hence, the

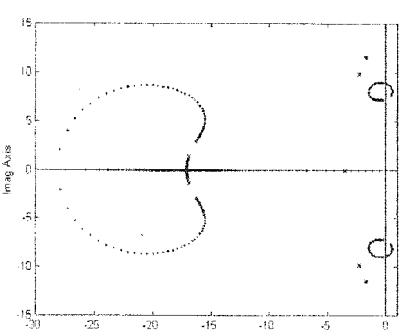

Figure 4. Root locus for case 1 $k\omega$ changes from 0 to 10.2.

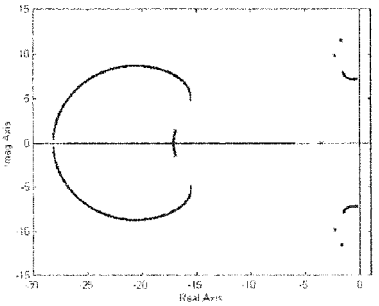

Figure 5. Root locus for case 2 $k\omega$ changes from 0 to 500.

speed of movement of eigenvalues will be increased (decreased) in lower (higher) frequencies. Frequency dependence of LOADSYN model is more than exponential model, therefore the speed of eigenvalue movement of LOADSYN model is more than exponential model for $\omega < 1$ (as shown in Figures 4 and 5) and less than exponential model for $\omega > 1$.

Figures 4 and 5 show that the damping of critical eigenvalues will be increased if $k\omega$ increases a small value, although it will be deceased if $k\omega$ increases greatly. They also show that one eigenvalue moves toward the right of imaginary axis and may make the system unstable if $k\omega$ increases greatly.

When $k\omega$ equals zero, load is not frequency dependent, and there are only 12 eigenvalues. If $k\omega = +0 (k\omega = -0)$, an eigenvalue will be added at minus infinity (plus infinity) and move toward the imaginary axis as $k\omega$ increases (decreases). Equations (30) and (31) and Figure 6 show that in case 3, $t1_{ll}$ and $t2_{ll}$ remain constant, $m1_{ll}$ and $m2_{ll}$ increase, and critical eigenvalues move toward the left of imaginary axis as k_v increases, therefore the locations of critical eigenvalues depend only on the values of $m1_{ll}$ and $m2_{ll}$.

The infinite bus was modeled using two methods, directly and through a large generator; the cpu time that is needed for calculating K coefficients in the first method is 1.5 times less than the second method in this example. The defined K coefficients are given for a specified operating point in appendix B.

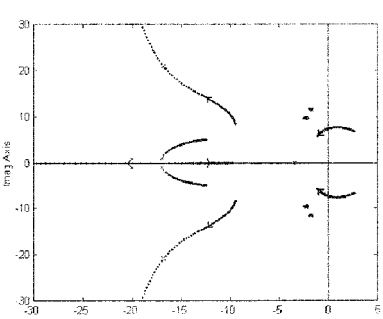

Figure 6. Root locus for case 3 kv change from -100 to 100.

3.2 Designing PSS

For a one-machine infinite bus with frequency- and voltage-dependent local load, parameters and operating point are given in Appendix C. If the load is considered as an impedance load, then

K1	K2	K3	K4	K5	K6
1.6494	2.0267	0.3227	1.3051	0.0105	0.6636

If the desired damping ratio is $\xi = 0.3$, designing PSS based on complex frequency yields ($G_{pss}(s) = Kc(1 + T_1 s)/(1 + T_2 s)$):

Mechanical mode	Phase lag of electrical loop	T2	T1	Kc
−0.1730 + 9.8872i	−38.5899	0.1000	0.7979	2.5042

Now, for a LOADSYN model for the local load with $kpv = 0.1$, $kp\omega = 2.6$, $kqv = 0.6$ and $kq\omega = 1.6$, which are typical parameters of an industrial load [14], kp and kq are chosen such that active and reactive loads are equal to active and reactive loads at operating point. Then

K1	K2	K3	K4	K5	K6	K′1	K′4	K′5	N″2	S″2	R″2
4.19	2.829	0.264	3.627	−0.034	0.658	−4.226	−3.864	0.074	−1011	610	358

Designing PSS for power systems with voltage- and frequency-dependent load is completely similar to designing PSS for power systems with impedance load

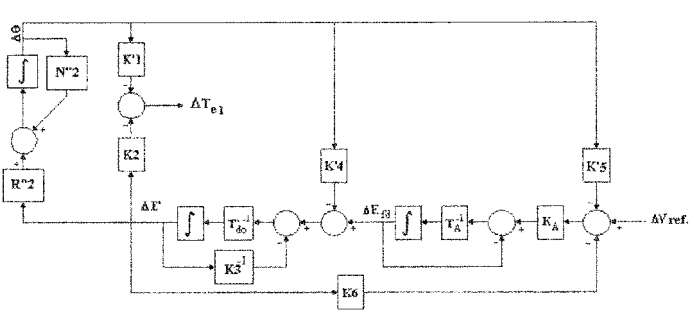

Figure 7. Electrical loop for frequency dependent load machine.

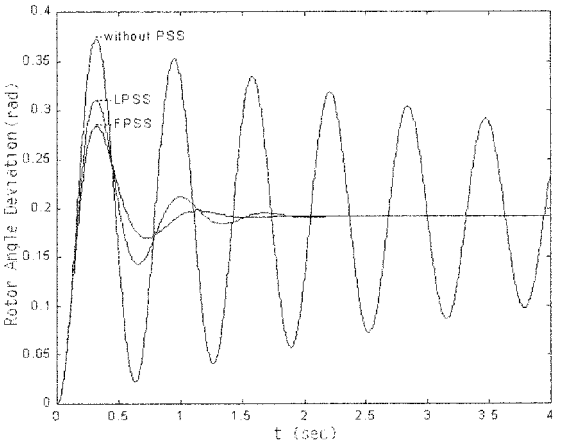

Figure 8. Rotor angle deviation.

except the electrical loop in this case is as in Figure 7. If the desired damping ratio is $\xi = 0.3$, designing PSS based on complex frequency yields ($G_{pss}(s) = Kc(1 + T_1 s)/(1 + T_2 s)$):

Mechanical mode	Phase lag of electrical loop	T2 T2	T1 T1	Kc Kc
−0.1889 + 9.9527i	−37.8784	0.1000	0.7353	4.1481

To compare the effects of above PSSs, a step $\Delta P_m = 0.3$ is applied. Rotor angle deviation for system without PSS, system with PSS designed based on impedance load (LPSS), and system with PSS designed based on frequency- and voltage-dependent load (FPSS) is shown in Figure 8. This figure shows that the performance of FPSS is quite better than LPSS.

4 Conclusion

A systematic method for driving the state equations of linear state space models for multi-machine power systems with voltage- and frequency-dependent loads was proposed. The state variables are the same as those of the Heffron-Phillips model for multi-machine power systems with impedance load plus the voltage angles of buses with frequency-dependent loads. The resulting block diagram is very similar to Heffron-Phillips model and is suitable for generalizing dynamic studies of networks with impedance loads to networks with frequency-dependent loads. It can be used for designing PSS, coordinating PSSs, determining an optimal place for PSSs, and determining the effects of loads on dynamic stability in a power system with frequency- and voltage-dependent loads. A simple method to account

for infinite bus was proposed. As an example, the effects of load model parameters on locus of critical eigenvalues for a five-bus network were studied. A PSS was designed for a one-machine infinite bus with frequency- and voltage-dependent local load. Comparison shows that the performance of the PSS design based on frequency-dependent load is quite better than PSS design based on impedance load.

References

[1] W. G. Heffron and R. A. Phillips, 1952, "Effect of a Modern Amplidyne Voltage Regulator on Underexcited Operation of Large Turbine Generators," *AIEE Trans. PAS*, Vol. 71, pp. 692–697.
[2] F. P. de Mello and C. Concordia, 1969, "Concepts of Synchronous Machine Stability as Affected by Excitation Control," *IEEE Trans. PAS*, Vol. 88, No. 4, pp. 316–329.
[3] F. P. de Mello and T. F. Laskowski, 1975, "Concepts of Power System Dynamic Stability," *IEEE Trans. PAS*, Vol. 94, No. 3, pp. 827–833.
[4] Y.-N. Yu, 1983, *Electric Power System Dynamics*, Academic Press, New York.
[5] F. P. de Mello, P. J. Nolan, T. F. Laskowski, and J. M. Undrill, 1980, "Co-ordinated Application of Stabilisers in Multi-machine Power Systems," *IEEE Trans. PAS*, Vol. 99, No. 3, pp. 892–901.
[6] R. J. Fleming, M. A. Mohan, and K. P. Parvatisam, 1981, "Selection of Parameters of Stabilisers in Multi-machine Power Systems," *IEEE Trans. PAS*, Vol. 100, pp. 2329–2333.
[7] H. B. Gooi, E. F. Hill, M. A. Mobarak, D. H. Throne, and T. H. Lee, 1981, "Co-ordinated Multi-machine Stabiliser Settings Without Eigenvalue Drift," *IEEE Trans. PAS*, Vol. 100, pp. 3879–3886.
[8] S. Abe and A. Doi, 1981, "A New Power System Stabiliser Synthesis in Multi-machine Power Systems," *IEEE Trans. PAS*, Vol. 102, pp. 3910–3918.
[9] A. Dio and S. Abe, 1984, "Co-ordinated Synthesis of Power System Stabilisers in Multi-machine Power Systems," *IEEE Trans. PAS*, Vol. 103, No. 6, pp. 1473–1476.
[10] O. H. Abdalla, S. A. Hassan, and N. T. Tweing, 1984, "Co-ordinated Stabilisation of a Multi-machine Power System," *IEEE Trans. PAS*, Vol. 103, No. 3, pp. 483–494.
[11] C. J. Berg, 1973, "Power System Load Representation," *Proc. IEEE*, Vol. 120, No. 3, pp. 344–348.
[12] General Electric Company, 1987, Load Modelling for Power Flow and Transient Stability Computer Studies, EPRI Final Report EL-5003.
[13] W. W. Price, K. A. Wirgau, A. Murdoch, J. V. Mitsche, E. Vaahedi, and M. A. El-Kady, 1988, "Load Modelling for Power Flow and Transient Stability Computer Studies," *IEEE Trans. PWRS*, Vol. 3, No. 1, pp. 180–187.
[14] IEEE Committee Report, 1993, "Load Representation for Dynamic Performance Analysis," *IEEE Trans. PWRS*, Vol. 8, No. 2, pp. 472–482.
[15] M. Brucoli, M. La Scala, R. Sbrizzai, and M. Trovato, 1993, "Voltage Stability Analysis of Electric Power Systems with Frequency Dependent Loads," *IEE Generation, Transmission and Distribution*, Vol. 140, No. 1, pp. 1–6.
[16] W. S. Kao, C. J. Lin, C. T. Huang, Y. T. Chen, and C. Y. Chiou, 1994, "Comparison of Simulated Power System Dynamics Applying Various Load Models with Actual Recorded Data," *IEEE Trans. PWRS*, Vol. 9, No. 1, pp. 248–254.
[17] IEEE Committee Report, 1995, "Bibliography on Load Models for Power Flow and Dynamic Performance Simulation," *IEEE Trans. PWRS*, Vol. 10, No. 1, pp. 523–538.

[18] W. S. Kao, C. T. Huang, and C. Y. Chiou, 1995, "Dynamic Load Modelling in TaiPower System Stability Studies," *IEEE Trans. PWRS*, Vol. 10, No. 2, pp. 907–914.
[19] IEEE Committee Report, 1995, "Standard Load Models for Power Flow Dynamic Performance Simulation," *IEEE Trans. PWRS*, Vol. 10, No. 3, pp. 1302–1313.
[20] I. A. Hiskens and J. V. Milanovic, 1995, "Load Modelling in Studies of Power System Damping," *IEEE Trans. PWRS*, Vol. 10, No. 4, pp. 1781–1788.
[21] B. Khodabakhchian and G. T. Vuong, 1997, "Modelling a Mixed Residential-Commercial Load for Simulations Involving Large Disturbances," *IEEE Trans. PWRS*, Vol. 12, No. 2, pp. 791–796.
[22] K. Tomiyama, J. P. Daniel, and S. Ihara, "Modelling Air Conditioner Load for Power System Studies," *http://www.ieee.org/organizations/society/power/subpages/abstract-folder/abs997.htm*
[23] T. S. Bhatti and D. J. Hill, 1990, "A Multi-machine Heffron-Phillips Model for Power Systems with Frequency and Voltage Dependent Loads," *IEEE Trans. Electrical Power & Energy Systems*, Vol. 12, No. 3, pp. 171–182.
[24] O. I. Elgerd, 1982, *Electric Energy Systems Theory: An Introduction*, New York, McGraw-Hill.
[25] M. Oloomi Buygi, 1993, *Low Frequency Oscillations Analysis in Power Systems with Voltage and Frequency Dependent Loads*, B.S. Thesis, Ferdowsi University.

Appendix A: Five Buses Example Data

Machine data

Gen. no.	Rating (MVA)	Inertia H(sec)	Damping (pu)	Xd = Xq (pu)	X′d (pu)	External reactance (pu)	TA (sec)	KA
1	166.6	4.3	0	1.164	0.146	0.0194	0.02	153.3
2	166.6	4.3	0	1.029	0.126	0.0194	0.05	287.4
3	325	10.35	0	0.625	0.084	0.0327	0.02	324
Inf. B.	—	1000	—	0.0001	0.00001	0.067	—	—

Operating condition

Bus no.	Pg (MW)	Qg (MVAR)	Pl (MW)	Ql (MVAR)	V (pu)	θ (deg)
1	90	27.55	0	0	1.02	10.66
2	90	27.55	0	0	1.02	10.66
3	175	20.51	0	0	1.02	12.86
4	0	0	100	20	1.015	9.69
5	2000	300	2255	300.6	1	0

Appendix B: Example Coefficients for Application 1

The defined coefficients for above operating point and $k\omega = 1, kv = 2, \omega = 1$ are as follows:

K1

3.1382e+00	−8.4080e−02	−4.8249e−02
−7.8430e−02	3.2705e+00	−5.7694e−02
−7.2048e−02	−9.2361e−02	5.4036e+00

K2

3.5659e+00	−3.0156e−01	−2.9305e−01
−2.9704e−01	3.7830e+00	−3.5043e−01
−2.7286e−01	−3.3126e−01	5.9500e+00

K3

1.5519e−01	−1.1577e+00	−1.1914e+00
−1.3244e+00	1.5638e−01	−1.1226e+00
−2.1100e+00	−1.7380e+00	1.9697e−01

K4

3.6951e+00	−2.4081e−01	−1.3819e−01
−1.9935e−01	3.4944e+00	−1.4665e−01
−1.2513e−01	−1.6041e−01	3.3010e+00

K5

6.9568e−02	4.5997e−02	2.6395e−02
3.5216e−02	8.5279e−02	2.5906e−02
3.2426e−02	4.1568e−02	9.3952e−02

K6

2.2898e−01	1.6497e−01	1.6031e−01
1.3337e−01	2.7291e−01	1.5734e−01
1.2880e−01	1.4909e−01	3.4988e−01

K′1

−3.0327e+00
−3.1665e+00
−5.2687e+00

K′4

−3.3929e+00
−3.2299e+00
−3.0667e+00

K′5

−1.2728e−01
−1.3199e−01
−1.5468e−01

R″2 lf.gn

8.8006e+02	8.8480e+02	1.762e+03

S″2 lf.gn

1.0604e+03	1.0820e+03	1.9487e+03

N″2 lf.lf

−9.7829e+03

Appendix C: Parameters and Operating Point of Application 2

Gen.: M = 6 sec, D = 0, T'do = 2 sec, r = 0, xd = 1.15 pu, x'd =0.15 pu, xq = 0.6 pu.
Exc.: $K_A = 40$, $T_A = 0.02$ sec.
Line: Rl = 0, xl = 0.4 pu, Gl = 0, Bl = 0.
Operating point: Pg = 1.5 pu, Qg = 0.8208 pu, Pd = 1 pu, Qd = 0.5 pu, Vinf. = 1.